Available online at www.sciencedirect.com
ScienceDirect
Journal of Inorganic Biochemistry 100 (2006) 2009–2016
Journal of Inorganic Biochemistry
www.elsevier.com/locate/jinorgbio

Redox chemistry of low-pH forms of tetrahemic cytochrome c_3

M. Santos [a], M.M. Correia dos Santos [a], M.L. Simões Gonçalves [a], C. Costa [c], J.C. Romão [b], J.J.G. Moura [c,*]

[a] *Centro de Química Estrutural, Instituto Superior Técnico, Av. Rovisco Pais, 1049-001 Lisboa, Portugal*
[b] *Centro de Física Teórica de Partículas, Instituto Superior Técnico, Av. Rovisco Pais, 1049-001 Lisboa, Portugal*
[c] *REQUIMTE, Centro de Química Fina e Biotecnologia, Departamento de Química, Faculdade de Ciências e Tecnologia, Universidade Nova de Lisboa, 2829-516 Caparica, Portugal*

Received 21 June 2006; received in revised form 13 September 2006; accepted 14 September 2006
Available online 23 September 2006

Abstract

Desulfovibrio vulgaris Hildenborough cytochrome c_3 contains four hemes in a low-spin state with bis-histidinyl coordination. High-spin forms of cytochrome c_3 can be generated by protonation of the axial ligands in order to probe spin equilibrium (low-spin/high-spin). The spin alterations occurring at acid pH, the associated changes in redox potentials, as well as the reactivity towards external ligands were followed by the conjunction of square wave voltammetry and UV–visible, CD, NMR and EPR spectroscopies. These processes may be used for modelling the action of enzymes that use spin equilibrium to promote enzyme activity and reactivity towards small molecules.

Keywords: Multiheme cytochromes; High/low-spin transitions; Reactivity with external ligands; Electrochemistry; Spectroscopy

1. Introduction

Class III cytochromes are multiheme electron transfer proteins isolated in the redox system of anaerobic bacteria, namely sulphate- and sulphur-reducers. The members of the family have in common hemes that attain a low-spin iron configuration with bis-histidinyl coordination with quite negative redox potentials (−0.200 to −0.600 V *vs* Ag/AgCl), when compared with mitochondrial cytochrome *c* (+0.045 V *vs* Ag/AgCl, Met–His heme axial coordination). Several members of the family have been identified. Tetrahemic cytochromes c_3 (13 kDa) are the most abundant. The family is large and comprises dimeric diheme [1], dimeric tetraheme [2], monomeric 9 heme [3] and monomeric 16 heme proteins [4]. A very tight control of the redox potentials of the hemes by protonation has been extensively described in different members of the family with relevance for proton–electron coupled reactions (redox-Bohr effect) [5]. The axial His ligands can also be protonated affecting the redox properties, the spin states and the reactivity of the hemes [6].

Electron transfer processes are essential for many metabolic performances, such as respiration and photosynthesis, just an example of two processes that are crucial for biosphere equilibrium. Heme proteins participate in such processes and are well characterized in terms of 3D structures [7,8].

The heme structure is a versatile arrangement of iron and ligands (equatorial and axial) that determine the overall reactivity. Mitochondrial cytochrome *c* has Met–His coordination that provides a strong ligand field to the heme site, except in extreme pH conditions, and reacts slowly with external ligands. However globins with weak ligand fields are highly reactive towards small molecules. Multiheme cytochromes c_3 have hemes in low-spin states with bis-His coordination. However these molecules are able

* Corresponding author. Tel.: +351212948382; fax: +351212948550.
E-mail address: jose.moura@dq.fct.unl.pt (J.J.G. Moura).

0162-0134/$ - see front matter © 2006 Elsevier Inc. All rights reserved.
doi:10.1016/j.jinorgbio.2006.09.013

to react with carbon monoxide and imidazole. The axial His ligands can be protonated, affecting the redox, the spin states and reactivity of the hemes. Cytochrome c_3 isolated from *Desulfovibrio vulgaris* Hildenborough is a representative member of the family.

Several published works document well the use of a wide range of electrochemical methods (differential pulse polarography and voltammetry, linear sweep and cyclic voltammetry) and different electrode systems (mercury, gold, carbon) in the study of redox potentials and electron transfer activity of cytochrome c_3 isolated from *D. vulgaris* [9–14]. In this work square wave voltammetry (SWV) and a membrane electrode were used to probe heme spin equilibrium associated with changes in the redox potentials of tetrahemic *D. vulgaris* Hildenborough cytochrome c_3 (*Dv* cyt c_3). Since the square wave voltammograms obtained correspond to four successive one-electron processes, the experimental data were fitted to the theoretical predictions for four similar but non-equivalent redox sites.

High-spin forms of *Dv* cyt c_3 were generated by protonation of the axial histidine ligands in order to probe spin equilibrium (high/low), as well as to generate putative reactive species towards external ligands. The spin alterations occurring at extreme pH, the associated changes in redox potentials, as well as the reactivity towards external ligands (NO) were complementary studied by the conjunction of UV–visible, CD, NMR and EPR spectroscopies and electrochemistry.

These processes may be used for modelling the action of enzymes that use spin equilibrium to promote enzyme activity (i.e., nitrite reductase cytochrome cd_1 [15,16] or di-heme cytochrome *c* peroxidase [17,18]).

2. Material and methods

Dv cyt c_3 was isolated as previously described [19].

All chemicals used were of pro-analysis grade and the solutions were made up with deionized water from a Milli-Q water purification system.

UV–visible spectra were recorded either in a Hewlett–Packard Diode Array Spectrophotometer 8452A or a Shimadzu UV-160A recording spectrophotometer at room temperature. EPR spectra were recorded in a Bruker ESP 300E spectrometer equipped with an Oxford Instruments continuous flow cryostat. NMR spectra were recorded in a Bruker 400 ARX instrument. For NMR experiments, samples were dialysed and exchanged with D_2O after liophylization. pH alterations were made by addition of minor amounts of acid or base as convenient (DCl or NaOD for NMR, with pD isotopic corrections introduced in the values reported).

Circular dichroism spectra were measured using a cylindrical 1 mm Hellma Quartz Suprasil cuvette, on a Jasco J-720 spectropolarimeter in the wavelength range 185–300 nm and 300–650 nm, at room temperature. The measuring conditions were: band width, 0.5 nm; response, 2 s; scanning speed, 50 nm/min. Each CD spectrum represents the average of at least three scans obtained by collecting data at 0.5 nm intervals. The analysis of the circular dichroism spectra for the determination of protein secondary structure was carried out using the CD spectra deconvolution program, CDNN version 2.1. The baseline obtained with water was subtracted from the sample spectra [20].

Square wave (SW) voltammetric measurements were performed using a potentiostat/galvanostat from ECO-Chemie, Autolab/PSTAT 10 as the source of applied potential and as a measuring device (data processed by the GPES software package from ECO-Chemie). The SW parameters were: square wave amplitude, E_{SW}, 50 mV, step height, ΔE_{SW} 5 mV and the frequencies varied between 10 and 200 Hz. The electrochemical cell featured a conventional three-electrode configuration. The reference electrode was a silver/silver chloride and the auxiliary electrode was a platinum wire. Two working electrodes were used: a glassy carbon electrode (GCE) from BAS (ref. MF-2012) with nominal radius = 0.15 cm and a gold electrode (AuE) with nominal radius = 0.08 cm also from BAS (ref. MF-2014). Prior to each experiment the electrodes were polished by hand on a polishing cloth (BUEHLER 40-7212) with water + alumina (0.05 μm) slurry (BUEHLER 40-6365-006), sonicated during 5 min and then rinsed well with Milli-Q water. In the experiments with the membrane-entrapped solution of the protein, the membrane electrodes (MGCE and MAuE) were prepared as followed: a small volume (2 μl) of the protein solution was deposited on a square piece (about twice the diameter of the electrode sensor) of the dialysis membrane (Spectra/Por MWCO 6000–8000, a negatively charged membrane), then the polished electrode was pressed against the membrane and a rubber ring was fitted around the electrode body so that the entrapped solution formed a uniform thin layer with thickness *l*. The membrane electrode was then placed in the three-electrode cell containing the supporting electrolyte, 100 mM sodium nitrate. Since small ions easily diffuse through the membrane, pH alterations were made by addition of acid or base as convenient to the cell containing the supporting electrolyte. Before each measurement the solutions were deaerated with U-type nitrogen that had been previously passed through the supporting electrolyte and then saturated with water. All measurements were done in a temperature-controlled room at $T = 24 \pm 1$ °C. All potential values are referred to Ag/AgCl electrode. Potentials versus the standard hydrogen electrode (SHE) can be obtained by adding 0.205 V.

NO reacted samples were generated as follows. EPR data was obtained by reacting HS forms (low pH) in a dithionite solution that contained nitrite (NO was generated locally). In electrochemistry, NO was generated in a separated vessel by reacting nitrite and dithionite and then allowed to bubble directly into the reaction vessel containing oxidized protein.

3. Results and discussion

3.1. pH dependent spin transitions followed by visible, circular dichroism, ^1H NMR and EPR spectroscopies

High/low-spin transitions due to the protonation/deprotonation of the axial histidine ligands of *Dv* cyt c_3 are observed to be a fully reversible process as concluded by visible absorption, circular dichroism and voltammetry (see below).

Fig. 1 (I, II and III) demonstrates the spin transition occurring by decreasing pH. The protein shows to be remarkably stable in a wide range of pH values. At acidic pH, a band at 630 nm clearly develops indicative of the presence of a high-spin form, with concomitant disappearance of the low-spin contributions (circa 500–600 nm region). The high-spin form is also characterized by a Soret absorption band at 360 nm. Superimposed spectra are obtained from protein solutions at basic pH (pH 9) and brought to that value from a solution initially at pH 1. The reversibility was demonstrated shuttling the protein within extreme pH values.

We also characterized the protein folding by circular dichroism at extreme pH values. Supporting the visible data, the main secondary structure elements are maintained at neutral and acidic pH (Table 1).

The spin transition was also clearly followed by EPR and NMR.

Dv cyt c_3 shows a rhombic low-spin EPR spectrum, with characteristic resonances in the spectral $g = 3$ region, at high pH values (Fig. 2A). However, at pH values below

Table 1
Elements of secondary structure extracted from circular dichroism measurements on *D. vulgaris* cytochrome c_3 at neutral and acidic pH values, in the 195–260 nm spectral region

	Native	pH 1.45	pH 6.45
Helix (%)	10.20	7.80	9.40
Antiparallel (%)	31.00	33.30	32.60
Parallel (%)	5.00	4.60	5.00
Beta-turn (%)	21.50	21.70	21.40
Random coil (%)	34.20	35.50	34.10
Total sum (%)	101.90	102.90	102.60

The native sample was placed at acidic condition and then the pH adjusted at 6.45 for reversible check.

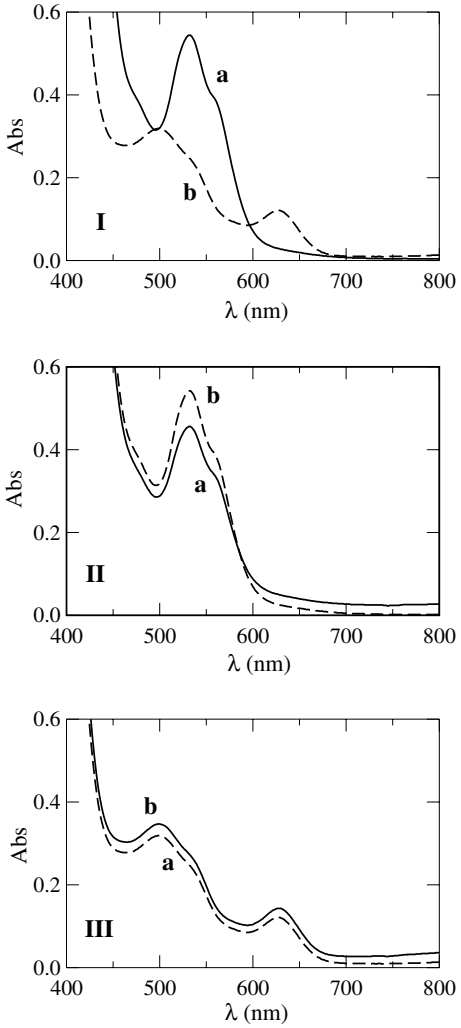

Fig. 1. UV–visible absorption spectra of the oxidised form of 0.013 mM *D.vulgaris* Hildenborough cytochrome c_3: (I) – (a) neutral and (b) acidic pH. The band at 630 nm is indicative of the presence of a high spin form. (II) pH 9 (a) and from a solution brought to pH 9, initially at pH 1 (b); (III) pH 1 (a) and from a solution brought to pH 1, initially at pH 9 (b). Medium: 100 mM sodium nitrate.

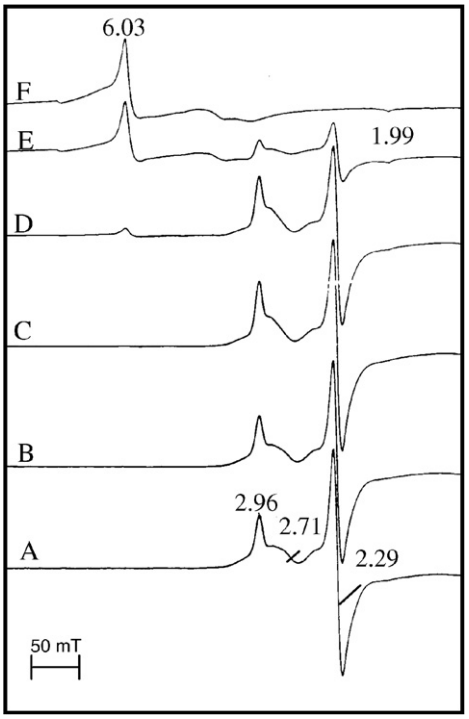

Fig. 2. EPR spectra of the 0.20 mM *D.vulgaris* Hildenborough cytochrome c_3 at different pH values. A – Native form (low spin) at pH 6.68, B – pH 4.80, C – pH 3.01, D – pH 2.60, E – pH 2.43, F – High spin form at pH 1.48. Experimental conditions: $T = 9$ K, microwave power 2 mW, field modulation 1 mT, $\upsilon = 9.44$ GHz, spectral width 0.5 T. *g*-values are shown in the figure.

2.5, the spectra indicate the presence of two EPR active species. In addition to the previously described low-spin species, a novel one develops associated with a well known axial high-spin EPR spectrum, with two g-values at 6 and 2, the ground state of a Kramer system of $S = 5/2$ (Fig. 2F) [21]. The low-spin contribution is absent at low pH values. This interpretation is also supported by NMR studies (data not shown). At high pH values, the *Dv* cyt c_3 shows a typical low-spin NMR spectrum, with the chemical shifts of the heme methyl groups situated at 10–30 ppm and presenting narrow line widths. On the other hand, the NMR spectrum of the totally reduced form has diamagnetic properties leading to the conclusion of the presence of a low-spin form [22]. With the decrease of the pH values, these resonances are substituted by enlarged bands, with chemical shifts in the low field region of 80 ppm that indicate a transition to a high spin state ($S = 5/2$), supporting the hypothesis of the axial ligand protonation. The NMR data shows the co-existence of low-spin and high-spin forms in intermediate pH values in a slow exchange regime in the NMR time scale.

3.2. pH dependent spin transitions followed by voltammetry

3.2.1. Electrochemical behaviour

A direct and reproducible voltammetric result was obtained for the reduction of *Dv* cyt c_3 at either the GCE and AuE or the MGCE and MAuE in a wide range of pH values. Due to the closeness of redox potentials a single peak is observed [9–14] with half peaks width at half high $W_{1/2} = 150$ mV, larger than expected for a one electron reversible reaction (23). The wave forms in all experimental conditions were carefully analyzed in terms of peak potential and half peak width as a function of the frequency, as well peak current with the square root of frequency. The constancy of potentials over the frequency range analyzed as well the linear dependency (with a null intercept) of the peak currents with $(f)^{1/2}$ shows that the electrode reaction is reversible and diffusion controlled. This is true for the net as well as for the forward and reverse voltammograms. Analysis of the SW voltammograms was made in terms of diffusion-controlled process even in the case where the membrane electrode is used since the diffusion layer thickness is always smaller than the thickness of the entrapped solution l, as previously demonstrated, even for the longest time scales used, i.e., $tp = 0.05$ s ($f = 10$ Hz) [23,24].

3.2.2. SW voltammograms simulation

In order to determine the individual redox potentials, calculation methods were developed by Bianco and Haladjian [25] and Sokol and Niki [26], applied to both linear scan and differential pulse polarography, and by Moreno [27] for cyclic voltammetry.

In this work and since the SW voltammograms correspond to four successive one-electron processes, the experimental data was fitted to the theoretical predictions for four superimposed 1-electron processes [28,29].

The current on the jth half-cycle, is given by

$$i_j = nFAC(D/\pi t_p)^{1/2} \sum_{m=1}^{j} \frac{Q_{m-1} - Q_m}{\sqrt{j - m + 1}} \tag{1}$$

where

$$Q_m = \frac{\varepsilon_m}{1 + \varepsilon_m} \tag{2}$$

$$\varepsilon_m = \exp\left[\frac{nF(E_m - E^{\mathrm{r}}_{1/2})}{RT}\right] \tag{3}$$

with $E^{\mathrm{r}}_{1/2}$ being the reversible half-wave potential and the potential E in the half cycle m is given by

$$E_m = E_i - \left[\frac{m+1}{2}\right]\Delta E_s + (-1)^m E_{\mathrm{SW}} \tag{4}$$

In each cycle k, the forward difference is given by

$$\Delta i_k = i_{2k-1} - i_{2k} \equiv \Delta i^{\mathrm{th}}(E_k, E^{\mathrm{r}}_{1/2}) \tag{5}$$

with

$$E_k = (E_{2k} + E_{2k-1})/2 \tag{6}$$

Experimentally one has M data points $(E_k, I^{\mathrm{exp}}_k)$ $(k = 1, \ldots, M)$ that must be fitted to a superposition of four voltammograms with different values of $E^{\mathrm{r}}_{1/2}$. To achieve this one constructs the theoretical function:

$$I^{\mathrm{th}}(E, N, E^{\mathrm{r}}_{1/2}(1), \ldots, E^{\mathrm{r}}_{1/2}(4)) = N \sum_{j=1}^{4} \Delta i^{\mathrm{th}}(E, E^{\mathrm{r}}_{1/2}(j)) \tag{7}$$

and fits the parameters N (a common normalisation) and the four half wave potentials $E^{\mathrm{r}}_{1/2}$(j) $(j = 1, \ldots 4)$ by minimising the χ^2 defined by

$$\chi^2 = \sum_{k=1}^{M} \left[\frac{I^{\mathrm{exp}}_k - I^{\mathrm{th}}(E_k, N, E^{\mathrm{r}}_{1/2}(1), \ldots, E^{\mathrm{r}}_{1/2}(4))}{\Delta I_k}\right]^2 \tag{8}$$

where ΔI_k is the experimental error on the current I^{exp}_k.

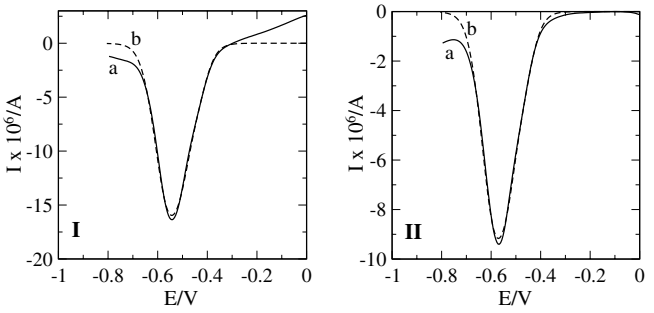

Fig. 3. Comparison of best fit SW voltammogram simulation for the reduction of *D. vulgaris* Hildenborough cytochrome c_3 at a glassy carbon electrode (a) experimental data; (b) simulation for four reversible redox centers. (I) without membrane, 0.33 mM cytochrome c_3; (II) with membrane, 1.6 mM cytochrome c_3; Other conditions: $f = 10$ Hz, $\Delta E = 5$ mV, $E_{\mathrm{SW}} = 50$ mV. Medium: 10 mM tris chloride buffer (pH 7) and 100 mM sodium nitrate.

Table 2
Formal potentials of reduction $E^{o'}$(V) *vs* Ag/AgCl, of *D.vulgaris* Hildenborough cytochrome c_3 at gold and glassy carbon electrodes, without and with membrane: Experimental and individual fitted values of the four hemes

	Gold electrode		Carbon electrode	
	Without membrane	With membrane	Without membrane	With membrane
Experimental	−0.54	−0.53	−0.54	−0.56
Heme 1	−0.47	−0.47	−0.47	−0.49
Heme 2	−0.53	−0.53	−0.54	−0.56
Heme 3	−0.53	−0.53	−0.54	−0.56
Heme 4	−0.60	−0.62	−0.59	−0.61

Medium 10 mM tris chloride buffer (pH 7) and 100 mM sodium nitrate.

Experimental and fitted voltammograms are shown for the reduction of *Dv* cyt c_3 on the glassy carbon electrode without (Fig. 3I) and with membrane (Fig. 3II). The individual fitted values for the formal potentials of reduction, $E^{o'}$, of the four hemes are presented in Table 2. In both situations very good fits were obtained and there is also a good agreement between the $E^{o'}$ values. Similar behaviour was observed with the gold electrode. Experimental and individual fitted $E^{o'}$ values at this electrode are also shown in Table 1 and, within the experimental error, they are in good agreement with the data obtained at the carbon electrode.

All further experiments were done with the protein solution entrapped between the electrode surface and the membrane in order to take advantage of the very tiny amounts of protein needed and how easily several experimental variables can be changed using the same unit [24].

In Fig. 4, the pH dependence of the SW peak current, I_p (Fig. 4I), and peak potential, E_p (Fig. 4II), is shown for cytochrome c_3 reduction at the membrane electrode. The variation observed for I_p follows previous results in particular the marked decrease for the extreme values of pH due to both changes in the protein charge and the overall electrode surface charge [27]. As to the peak potentials they remain fairly constant for pH values between 4 and 12. Changes in E_p towards more positive values occur with pH decreasing. In spite of these changes for extreme values of pH, no denaturation of the protein occurs. The voltammetric response obtained at e.g., pH 7 could always be restored either increasing or decreasing the solution pH. The same happened at the gold electrode (data not shown).

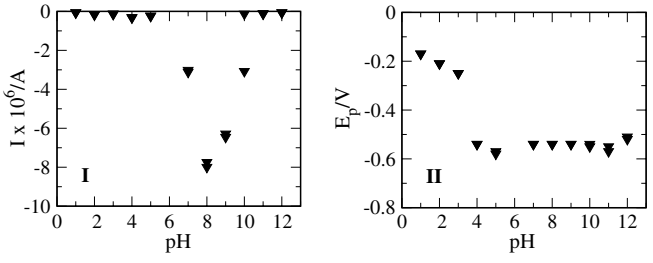

Fig. 4. pH dependence of the SW voltammogram peak current, I_p, (I) and peak potential, E_p, (II) for 1.6 mM *D. vulgaris* Hildenborough cytochrome c_3 at the membrane glassy carbon electrode. Other conditions: $f = 10$ Hz, $\Delta E = 5$ mV, $E_{SW} = 50$ mV. Medium: 100 mM sodium nitrate.

Simulation of the SW voltammograms permits to analyse the pH dependence of $E^{o'}$ of the four hemes of cytochrome c_3. As can be seen in Fig. 5 the reduction potential of all hemes is affected by the pH in agreement with structural and NMR data.

Upon pH decreasing and due to the protonation of the axial histidinyl ligands low-spin (LS)/high-spin (HS) transitions occur in the heme iron of cytochrome c_3. The effect of these transitions in the reduction potentials of the hemes is significant as shown by the voltammetric data. The reduction potential of each heme for the forms totally in low and high spin can be computed assuming that the alteration of the spin state of the heme iron is described by the reaction:

$$LS + H^+ \Longleftrightarrow HS$$

with equilibrium constant, K_a:

$$K_a = ([LS][H^+])/[HS] \quad (9)$$

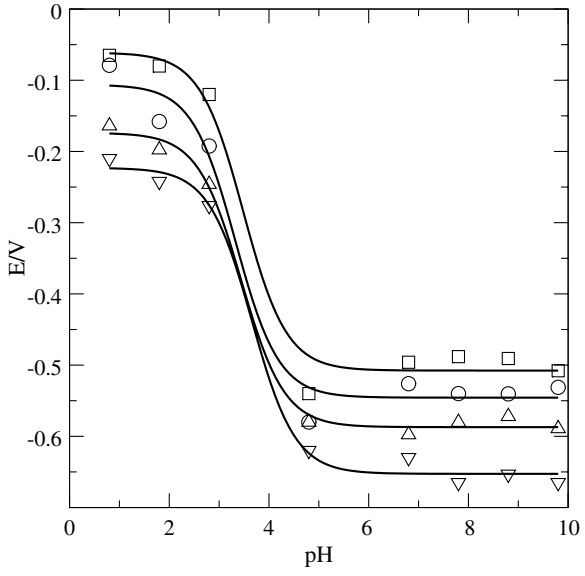

Fig. 5. pH dependence of the reduction potentials of the four hemes of *D. vulgaris* Hildenborough cytochrome c_3 at the membrane glassy carbon electrode: (squares) heme 1; (circles) heme 2; (triangles) heme 3; (inverted triangles) heme 4. Line fitted according to Eq. (11). Medium: 1.6 mM cytochrome c_3 and 100 mM sodium nitrate.

where [LS] and [HS] are the concentrations of the low and high spin species of a given heme in cytochrome c_3.

If f is the molar fraction of the low spin state species of a given heme then Eq. (9) can be rewritten as

$$K_a = (f[H^+])/(1-f) \quad (10)$$

The reduction potential of a given heme for each pH can be considered a weighted average of both contributions of the species in high and low spin, i.e.:

$$E_n^{o\prime} = fE_n^{o\prime}(LS) + (1-f)E_n^{o\prime}(HS) \quad (11)$$

with $n = 1$, 2, 3 or 4 and $E_n^{o\prime}(LS)$, $E_n^{o\prime}(HS)$ the reduction potentials of the forms totally in low- and high-spin, respectively for each heme. The fitting of the experimental values of $E_n^{o\prime}$ for each pH to Eq. (11) allows the determination of $E_n^{o\prime}(LS)$, $E_n^{o\prime}(HS)$ as well as of pK_a for each heme of the tetrahemic cytochrome (Table 3). The results obtained at both electrodes, MGCE and MAuE are shown in Table 3. Different potentials as well as pK_a values were obtained, which reflects the different chemical environment of each heme.

3.3. NO reacted high-spin states

The effect of exogenous ligands, as NO, was study by EPR and visible spectroscopy. Fig. 6 shows the EPR spectrum for the *Dv* cyt c_3 where NO replaced the heme axial histidinyl ligand. The addition of NO to iron hemic proteins lead to the observation of an EPR active NO-iron complex with unique and distinctive spectroscopic properties [30]. The EPR results show that, when the axial position is available (after histidine protonation), the heme iron of the cytochrome c_3 complexes with NO, leading to the observation of a triplet hyperfine interaction spectrum, consistent with coupling of the $S = 1/2$ spin to a single ^{14}N nucleus.

The UV–visible spectroscopy (not shown) results also support the formation of a coordinate nitrosyl heme: a Soret band at 412–419 nm is indicative of this coordination mode [31]. The EPR and UV–visible spectroscopies show that, at low pH values, a high-spin species is formed that has the capacity of NO binding.

Table 3
Formal potentials of reduction of the forms of low spin *vs* Ag/AgCl, $E^{o\prime}$(LS), high spin $E^{o\prime}$(HS) and protonation constant ($pK_a \pm 0.1$) of the axial histidine ligands of the four hemes *D. vulgaris* Hildenborough cytochrome c_3

	Electrode	Heme 1	Heme 2	Heme 3	Heme 4
$E^{o\prime}$(LS)/V	Gold	−0.48	−0.51	−0.57	−0.62
	Carbon	−0.51	−0.54	−0.59	−0.65
$E^{o\prime}$(HS)/V	Gold	−0.16	−0.17	−0.25	−0.29
	Carbon	−0.06	−0.11	−0.17	−0.22
pK_a	Gold	3.0	3.1	3.5	3.8
	Carbon	3.5	3.3	3.4	3.7

Values calculated according to Eq. (11). Medium: 100 mM sodium nitrate.

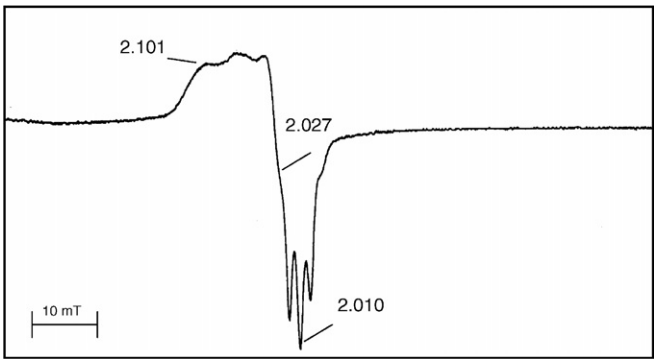

Fig. 6. Effect of the NO ligation to the high spin form: EPR spectra of the complex NO-heme iron of 0.20 mM *D. vulgaris* Hildenborough cytochrome c_3 at pH 1.5, after reduction with dithionite and subsequent addition of sodium nitrite. $T = 38$ K, microwave power 2.4 mW, field modulation 1 mT, $\upsilon = 9.44$ GHz, spectral width 0.1 T. g-values are shown in the figure.

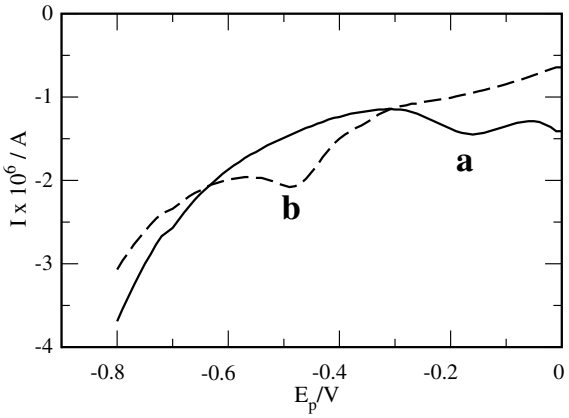

Fig. 7. Effect of the NO ligation to the high spin form: SW voltammograms of 1.3 mM *D. vulgaris* Hildenborough cytochrome c_3 at pH 1.5 (a) in the absence and (b) in the presence of NO. Other conditions: $f = 10$ Hz, $\Delta E = 5$ mV, $E_{SW} = 50$ mV. Medium: 100 mM sodium nitrate.

The electrochemical behaviour of cytochrome c_3 was also studied in the presence of NO. As can be seen in Fig. 7, upon addition of NO into the voltammetric cell at pH 1.5, there is a significant shift in the reduction peak potential from $E_p = -0.170$ V *vs* Ag/AgCl towards more negative potentials. The complex of *Dv* cyt c_3 with NO has a reduction potential of −0.480 V *vs* Ag/AgCl. Analysis of the square wave voltammograms revealed that the redox reaction becomes irreversible as could be concluded by the non-existence of the reverse current. No changes were observed in solutions of higher pH. These results show that at low pH values, when the protein is in the high-spin form, binding of NO occurs.

4. Conclusions

Two main roles are generally assigned to heme proteins: electron transfer, and catalysis of substrate molecules and consequently involvement in catalysis. Hexa-coordination

of the heme site prevents the possibility of substrate interactions. Empty coordination spheres or the presence of labile ligands facilitates the promotion of substrate-catalysed reactions. Also, it is well described that activation of heme containing proteins, in order to attain a ready state, may involve alteration of coordination sphere of the heme site. Clearly, the so-called EC mechanisms (an electron transfer step followed by a chemical reaction) operate and may be used for modelling the action of enzymes that use spin equilibrium to promote enzyme activity and heme reactivity towards small external molecules (i.e. nitrite reductase cytochrome cd_1 [15,16] or di-heme cytochrome *c* peroxidase [17,18]).

In this context, the coexisting low-spin and high-spin hemes may occur in enzymes in the native state, without the need of further activation steps. An example is the penta-heme nitrite reductase, a protein that contains 1 high spin heme penta-coordinated (the catalytic site) and 4 low-spin hemes involved in electron transfer that converts nitrite in ammonia, a six electron reduction step [32].

Square wave voltammetry in a wide pH range was used in this study to probe spin equilibrium and its effect in the redox potentials of the hemes *Dv* cyt c_3. Also redox properties of NO bound species were extracted. Complementary, spectroscopic tools support the spin transitions as well as the formation of a NO bound species when axial histidinyl residues are protonated. The literature is scarce in redox data on high-spin heme states and NO-heme bound species. Recently, for the first time, the determination of the reduction potential for low-pH conformers of cytochrome *c* was made in the absence of denaturants [33]. In this case spectroscopy supports, at acidic pH, the detachment of two strong heme ligands (Met and His) and their replacement by two water molecules. The alteration of redox potential observed upon spin change (native cyt *c*: +260 mV, immobilized native cyt *c*: +370 mV and immobilized "acidic" cyt *c*: +70 mV, *vs* SHE) correlated with the redox span observed, in this work, for the tetraheme cytochrome when neutral (low-spin) and acidic (high-spin) forms are considered. The redox potentials of the hemes reflect, in addition to other factors, the axial coordination. Cytochrome *c* (His–Met) has a positive $E^{o\prime}$ (circa +260 mV, *vs* SHE) and tetraheme cytochrome c_3 (His–His) a negative one (circa – 300 mV, *vs* SHE). However, in acidic conditions, upon replacement of the axial native ligands by water molecules both types of hemes show quite similar redox potentials.

Another interesting aspect is the observation of the reversibility of the high-spin/low-spin transition, even when the protein is equilibrated at very acidic pH values. This indicates a remarkable stability of multiheme protein structure to adverse unfolding conditions. The redox potential of the hemes in the low-spin and high-spin configurations could also be determined (Table 3). Since the square wave voltammograms obtained correspond to four successive one-electron processes, the experimental data was fitted to the theoretical predictions for four similar but non-equivalent redox sites. Due to the good agreement between experimental and simulated data, the four hemes of cytochrome c_3 can be considered as non-equivalent with different midpoint potentials that span in a narrow range. The pK_a values observed for the spin transitions also indicate subtle differences related to heme environment, solvent heme exposure and/or orientation of the axial ligands determining non-equivalent heme sites as also (already) proved by NMR and EPR ([7], and references therein). The pK_a values estimated by visible absorption and EPR may be considered in reasonable agreement if we consider that the first measurements represent the contribution of all the hemes and the second a subset of hemes. However the pK_as estimated by voltammetric measurements can not be related directly. The electrochemistry measurements reflect the pK_as values of ferric and ferrous species (high and low spin). On the other end only ferric species are EPR detectable.

The binding of NO to the high-spin forms of *Dv* cyt c_3 indicates that low-spin/high-spin equilibrium may enhance the reactivity of the hemes towards the binding and eventually catalysis of small molecules.

Acknowledgements

We thank FCT-MCTES (POCTI/QUI/55543/2004) for financial support. I.Correia (CQE-IST) obtained the CD spectra here reported.

Appendix A. Supplementary data

Supplementary data associated with this article can be found, in the online version, at doi:10.1016/j.jinorgbio.2006.09.013.

References

[1] P.M. Matias, J. Morais, A.V. Coelho, R. Meijers, A. Gonzalez, A.W. Thompson, L.C. Sieker, J. LeGall, M.A. Carrondo, J. Biol. Inorg. Chem. 2 (1997) 507–514.
[2] P.M. Matias, R. Coelho, I.A. Pereira, A.V. Coelho, A.W. Thompson, L.C. Sieker, J. LeGall, M.A. Carrondo, Struct. Fold Des. 7 (1999) 119–130.
[3] M. Czjzek, F. Guerlesquin, M. Bruschi, R. Haser, Structure 4 (1996) 395–404.
[4] W.B. Pollock, M. Loutfi, M. Brushi, B.J. Rapp-Giles, J.D. Wall, G. Voordouw, J. Bacteriol. 173 (1991) 220–228.
[5] M. Coletta, T. Catarino, J. LeGall, A.V. Xavier, Eur. J. Biochem. 202 (1991) 1101–1106.
[6] P. Rydberg, E. Sigfridsson, U. Ryde, J. Biol. Inorg. Chem. 9 (2004) 203–223.
[7] P.M. Matias, I.A.C. Pereira, C.M. Soares, M.A. Carrondo, Prog. Biophys. Mol. Biol. 89 (2005) 292–329.
[8] G.R. Moore, G.W. Pettigrew, Cytochromes *c*: Evolutionary, Structural and Physicochemical Aspects, Springer-Verlag, Berlin, 1990.
[9] K. Niki, T. Yagi, H. Inokuchi, K. Kimura, J. Am. Chem. Soc. 101 (1979) 3335–3340.
[10] P. Bianco, J. Haladjian, Biochim. Biophys. Acta 545 (1979) 86–93.
[11] C. van Djik, J.W. van Leeuwen, C. Veeger, J.P.G.M. Schreurs, E. Barendrecht, Bioelectrochem. Bioenerg. 9 (1982) 743–759.
[12] C. Hinnen, R. Parsons, K. Niki, J. Electroanal. Chem. 147 (1983) 329–337.

[13] P. Bianco, A. Manjaqui, J. Haladjian, M. Bruschi, J. Electroanal. Chem. 249 (1988) 241–252.
[14] D. Zhang, G.S. Wilson, K. Niki, Anal. Chem. 66 (1994) 3873–3881.
[15] S.C. Baker, N.F. Saunders, A.C. Willis, S.J. Ferguson, J. Hajdu, V. Fulop, J. Mol. Biol. 269 (1997) 440–455.
[16] H. Lopes, R. Gilmor, G. Pettigrew, I. Moura, J.J.G. Moura, J. Biol. Inorg. Chem. 3 (1998) 643–649.
[17] H. Lopes, S. Besson, I. Moura, J.J.G. Moura, J. Biol. Inorg. Chem. 6 (2001) 55–62.
[18] W. Hu, G. Van Driessche, B. Devreese, C.F. Goodhew, D.F. McGinnity, N. Saunders, V. Fulop, G.W. Pettigrew, J.J. Van Beeumen, Biochemistry 26 (1997) 7958–7966.
[19] I.B. Coutinho, A.V. Xavier, Method. Enzymol. 243 (1994) 119–140.
[20] G. Böhm, R. Muhr, R. Jaenicke, Protein Eng. 5 (1992) 191–195.
[21] G. Palmer, Biochem. Soc. Trans 13 (1985) 548–560.
[22] R.O. Louro, I. Pacheco, D.L. Turner, J. LeGall, A.V. Xavier, Febs Lett. 390 (1996) 59–62.
[23] A.J. Bard, L.R. Faulkner, Electrochemical Methods, Fundamentals and Applications, John Wiley and Sons, New York, 2001.
[24] M.M.C. dos Santos, P.M.P. Sousa, M.L.S. Gonçalves, L. Krippahl, J.J.G. Moura, E. Lojou, P. Bianco, J. Electroanal. Chem. 541 (2003) 153.
[25] P. Bianco, J. Haladjian, Electrochim. Acta 8 (1981) 1001–1004.
[26] W.F. Sokol, D.H. Evans, K. Niki, T. Yagi, J. Electroanal. Chem. 141 (1980) 743–759.
[27] C. Moreno, A. Campos, M. Teixeira, J. Legall, M.I. Montenegro, I. Moura, C. van Dijk, J.J.G. Moura, Eur. J. Biochem. 202 (1991) 385–393.
[28] J. Osteryoung, J.J. O'Dea, Square wave voltammetry, in: A.J. Bard (Ed.), Electroanalytical Chemistry, Vol. 14, Marcel Dekker, New York, 1986, p. 209.
[29] M.M.C. dos Santos, M.L.S. Gonçalves, J.C. Romão, J. Electroanal. Chem. 413 (1996) 97–103.
[30] M.C. Liu, B.H. Huynh, W.J. Payne, H.D. Peck Jr., D.V. Dervartanian, J. Legall, Eur. J. Biochem. 169 (1987) 253–258.
[31] H. Iwasaki, T. Yoshimura, S. Suzuki, S. Shidara, Biochim. Biophy. Acta 1058 (1991) 79–82.
[32] M.G. Almeida, S. Macieira, L.L. Gonçalves, R. Huber, C.A. Cunha, M.J. Romão, C. Costa, J. Lampreia, J.J.G. Moura, I. Moura, Eur. J. Biochem. 270 (2003) 3904–3915.
[33] C.A. Borlotti, G. Battistuzzi, M. Borsari, P. Facci, A. Ranieri, M. Sola, J. Am. Chem. Soc. 128 (2006) 5445–5451.